Scalar mixing in a turbulent boundary layer

Eisma, Jerke; Tam, Daniel; Westerweel, Jerry; van de Water, Willem

Publication date
2018

Document Version
Final published version

Published in
Proceedings of the 19th International Symposium on Application of Laser and Imaging Techniques to Fluid Mechanics

Citation (APA)
Eisma, J., Tam, D., Westerweel, J., & van de Water, W. (2018). Scalar mixing in a turbulent boundary layer. In *Proceedings of the 19th International Symposium on Application of Laser and Imaging Techniques to Fluid Mechanics*

Scalar Mixing in a Turbulent Boundary Layer

J. Eisma[1], D. Tam[1], J. Westerweel[1,*], W. van de Water[1]
1: Laboratory for Aero- & Hydrodynamics, Delft University of Technology, The Netherlands
* Corresponding author: j.westerweel@tudelft.nl

Keywords: PIV, LIF, Uniform Concentration Zones

ABSTRACT

We present results on the analysis of measurements on the dispersion of a contaminant in a turbulent boundary layer. The contaminant is a fluorescent dye (Rh.-B) that was introduced in a turbulent boundary layer ($Re_\theta = 3050$) in a water channel. The velocity field was measured by means of tomographic PIV. Simultaneously, the concentration field was measured by means of laser-induced fluorescence (LIF). The LIF data clearly reveal uniform concentration zones with well-defined boundaries. These zones are extracted from the probability density function of the local concentration. The key question is what flow structures make up their boundaries, and how these uniform concentration zones are related to uniform momentum zones. We evaluate the Lyapunov exponents of the rate of separation of two close points while they are advected by the flow. Local maxima of the Lyapunov exponents are known to create temporary barriers for transport in two-dimensional flows. Alternatively, the boundaries of uniform concentration zones may also be formed by shear layers, which are local maxima of the shear vorticity. There is a striking concentration of both the Lyapunov exponent and the shear vorticity on real boundaries. The correlation with the Lyapunov field is the weakest of the two. However, the Lyapunov exponent is a Lagrangian average, extending over episodes where these boundaries were formed, whereas the shear vorticity is based on a planar cross section of the instantaneous velocity field.

The spreading of a contaminant in a turbulent boundary layer appears to be characterised by large regions of almost uniform concentration, delineated by sharp boundaries, across which the concentration displays a sudden jump. These regions are commonly referred to as "uniform concentration zones" and appear to have similarities to so-called "uniform momentum zones" (Meinhart & Adrian 1995) that are delineated by shear layers, or "internal interface layers" akin to the external turbulent/non-turbulent interface (Da Silva *et al.* 2014; Eisma *et al.* 2015). This is in sharp contrast to the common idea that the turbulence strongly mixes contaminants that are introduced in a turbulent flow, which is directly related to the local eddy diffusivity. Clearly, understanding this anomalous dispersion is of great practical relevance for predicting pollutant concentration fluctuations in the atmospheric turbulent boundary layer.

In this paper we present recent results on the analysis of measurements on the dispersion of a contaminant in a turbulent boundary layer. The contaminant is a fluorescent dye (Rhodamine B) that was introduced in a turbulent boundary layer in a water channel. The measurement section of the channel has a length of 5 m and a 60×60 cm2 cross section. The measurements are taken 3.5 m downstream from the location where the boundary layer is tripped, while the dye is injected 0.75 m upstream from the measurement location. The Reynolds number based on the momentum loss thickness is $Re_\theta = 3050$. The velocity field was measured by means of tomographic PIV in a volume of $L_x \times L_y \times L_z = 1.5\delta_{.99} \times 1.65\delta_{.99} \times 0.15\delta_{.99}$, with a boundary layer thickness of: $\delta_{.99} = 0.038\text{m}$. Simultaneously, the 3D concentration field was measured by means of laser-induced fluorescence (LIF) in five slices spanning the spanwise $L_z = 0.15\delta_{.99}$ dimension of the measurement volume. Time series were recorded at a frequency of 128 Hz ($\approx 6\delta_{.99}/U_\infty$) that each lasted for 3 s. A schematic of the optical configuration and profiles of the mean flow and concentration are shown in Fig. 1. Further experimental details are provided elsewhere (Eisma *et al.* 2015; Eisma 2017).

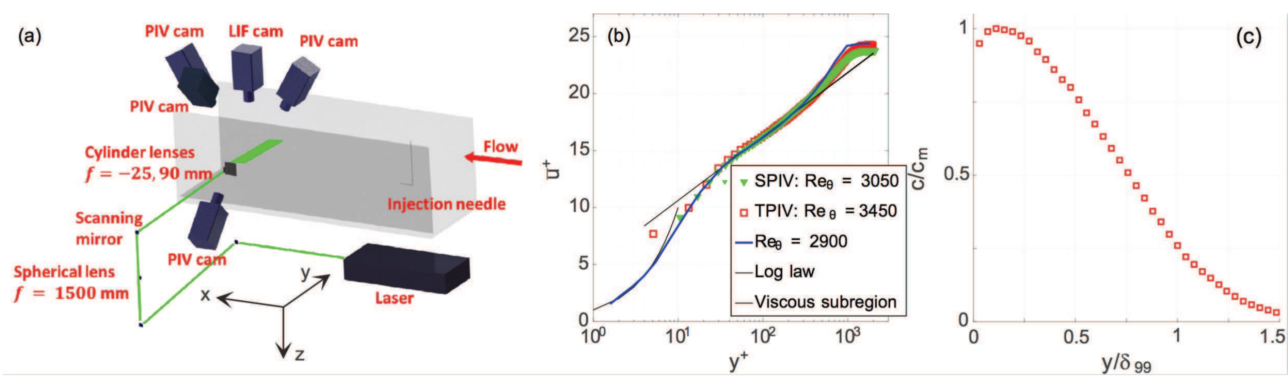

Fig. 1 (a) Schematic view of the experimental setup: tomographic PIV with 4 cameras and a scanning laser sheet; the volumetric concentration field of the tracer is registered using a single camera by means of LIF. (b) The measured mean turbulent velocity profile using tomographic PIV, compared to stereoscopic PIV measurements and results reported by DeGraaf & Eaton (2000), and the logarithmic wall layer. (c) Profile of mean dye concentration measured with LIF.

Uniform concentration zones can be recognised readily in the LIF snapshots of the center plane of the measurement volume shown in Fig. 2(a). From these snapshots, zones were extracted using an algorithm based on the probability density function of the local concentration; see Fig 2(d). In this example, four approximately contiguous uniform concentration zones with well-defined boundaries were extracted.

The emergence of these uniform concentration zones is a striking aspect of pollutant dispersion in a turbulent boundary layer. The key question is what flow structures make up their boundaries, and how these uniform concentration zones are related to uniform momentum zones. The measurements provide the full time-dependent three-dimensional velocity field of the flow, which allows the evaluation of sophisticated flow structures as candidates for concentration zone boundaries.

One of these is the rate of separation of two close points while they are advected by the flow. Local maxima of these spreading rates, or Lyapunov exponents $\Lambda(x)$, are known to create temporary barriers for transport in two-dimensional flows (Shadden *et al.* 2005). The Lyapunov field $\Lambda_{-T}(x)$ is shown in Fig.2(b), where the subscript $-T$ indicates the rate of spreading of points during a time T prior to arriving at x. Due to the advection by the mean velocity, the longest time interval over which trajectories could be integrated is $T \approx 2\delta_{.99}/U_\infty$.

Alternatively, the boundaries of uniform concentration zones may also be formed by shear layers (Eisma *et al.* 2015), which are local maxima of the shear vorticity ω_{sh} (Kolár 2007). Unlike the Lagrangian quantity $\Lambda_{-T}(x)$, ω_{sh} is evaluated from individual snapshots of the velocity field in a plane.

The correlation of these two fields, $\Lambda_{-T}(x)$ and $\omega_{\mathrm{sh}}(x)$, with the boundaries of uniform concentration zones is shown in Fig. 2(e). Of course, the fields $\Lambda_{-T}(x)$ and $\omega_{\mathrm{sh}}(x)$ are non-zero also inside the uniform concentration zones, so that we show the conditional average relative to one with artificial random boundaries. There is a striking concentration of both $\Lambda_{-T}(x)$ and $\omega_{\mathrm{sh}}(x)$ on real boundaries. It appears that the correlation with the Lyapunov field $\Lambda_{-T}(x)$ is the weakest of the two. However, it should be noted that $\Lambda_{-T}(x)$ is a Lagrangian average (directly related to the flow dynamics), extending over episodes where these boundaries were formed, whereas $\omega_{\mathrm{sh}}(x)$ is based on a planar cross section of the instantaneous velocity field (and thus describes only a kinematic feature of the flow).

Figure 2. (a) Snapshot of the concentration in the centre plane of the measurement volume ($z = 0$). (b) Lyapunov field $\Lambda_{-T}(x)$ corresponding to (a), which gauges the rate of separation of close points before they reach the observation window. The full time-dependent 3D velocity field was used for the computation of $\Lambda_{-T}(x)$. (c) Shear vorticity ω_{sh} which emphasises the shear component of the deformation rate measured in the centre plane of the measurement volume. (d) Same as (a), but after identification of 4 uniform concentration zones. The arrow indicates the direction of y in the conditional averages. (e) Full line shows the conditional average of $\Lambda_{-T}(x)$ across the boundaries of uniform concentration zones; the dashed line represents the conditional average of ω_{sh}.

References

Da Silva, C.B., Hunt, J.C.R., Eames, I. & Westerweel, J. (2014) Interfacial layers between regions of different turbulence intensity. Annu. Rev. Fluid Mech. 46:567-590

Eisma, J., Westerweel, J., Ooms, G. & Elsinga, G.E. (2015) Interfaces and internal layers in a turbulent boundary layer. Phys. Fluids 27:055103

Eisma, H.E. (2017) Pollutant Dispersion in Wall-Bounded Turbulent Flows. Ph.D. thesis, Delft University of Technology.

DeGraaf, D.B. & Eaton, J.K. (2000) Reynolds-number scaling of the flat-plate turbulent boundary layer. J. Fluid Mech. 422:319-346

Kolár, V. (2007) Vortex identification: New requirements and limitations. Int. J. Heat Fluid Flow 28:638-652

Meinhart, C.D. & Adrian, R.J. (1995) On the existence of uniform momentum zones in a turbulent boundary layer. Phys. Fluids 7:694-696

Shadden, S.C., Lekien, F. & Marsden, J.E. (2005) Definition and properties of Lagrangian coherent structures from finite-time Lyapunov exponents in two-dimensional aperiodic flows. Physica D 212:271-304